

Impacts of the African Humid Period termination may have been delayed in the Atlantic Sahara

Juliana Nogueira^{1,2}, Heitor Evangelista², Abdelfettah Sifeddine³, Ahmed ElMouden⁴,
Lhoussaine Bouchaou^{4,5}, Yassine Ait Brahim⁶, Mercedes Mendez-Millan³, Sandrine
Caquineau³, Patricia Piacsek⁷, Francisco Javier Briceño-Zuluaga⁸, Hugues Boucher³,
Moussa Masrour⁴, Lucie Juříčková⁹

¹ Faculty of Forestry and Wood Sciences, Czech University of Life Sciences Prague. Kamýcká 129. 165 00. Prague, Czech Republic

² LARAMG – Radioecology and Climate Change Laboratory, Department of Biophysics and Biometry, Rio de Janeiro State University. Rua São Francisco Xavier, 524. 20550-013. Rio de Janeiro, RJ, Brazil.

³IRD, Sorbonne Université, CNRS, MNHN, IPSL, LOCEAN, Bondy, France.

⁴ Laboratory of Applied Geology and Geo-Environment, Ibn Zohr University, Agadir, Morocco.

⁵ International Water Research Institute (IWRI), Mohammed VI Polytechnic University (UM6P), Ben Guerir, Morocco.

⁶ International Water Research Institute (IWRI), Mohammed VI Polytechnic University (UM6P), Hay My Rachid, 43150, Ben Guerir, Morocco.

⁷ Centro de Geociencias, Universidad Nacional Autónoma de México (UNAM), Blvd. Juriquilla 3001, Campus UNAM 3001, 76230 Juriquilla, Querétaro, México.

⁸ Facultad de Ciencias Básicas - Universidad Militar Nueva Granada, Bogotá, Colombia.

⁹ Department of Zoology, Faculty of Science, Charles University, Viničná 7, CZ-128 44 Praha 2, Czech Republic.

Corresponding author: snogueira.j@gmail.com, Twitter: @PaleoJuh

This paper is a non-peer reviewed preprint submitted to EarthArXiv and will be submitted soon to Communications Earth & Environment

ABSTRACT

The paleoenvironmental changes recorded at the Khnifiss Lagoon, on the Saharan Atlantic coast, southern Morocco, during the last 3.5 kyrs BP puts another piece to the puzzle on the intricate relationship between North Atlantic climate patterns and climate variations in Northwest Africa. This study shed light on the hydroclimatic dynamics during a pivotal climatic period: the transition from the mid- to late Holocene and the termination of the African Humid Period. Our research unveils two key periods of salt marsh expansion at the Khnifiss Lagoon, approximately 3.5 and 2.7 kyrs BP when humidity conditions and increased marine influence were recorded. Those conditions paint a scenario of increased storminess and precipitation in NW Africa, compatible with a negative NAO-like climatic configuration. Our data revealed a synchronization between this scenario in NW Africa and cooling events in the North Atlantic during the transition from the mid-to-late Holocene, related to Rapid Climate Changes (RCCs) occurring between 3.5 and 2.5 kyrs BP, also known as the Bond event #2. These findings can potentially enhance climate prediction models, offering opportunities to better prepare for and adapt to the evolving climate patterns in the region. High-resolution paleoenvironmental records are still rare in Northwest Africa and are highly needed. The knowledge gained from these studies represents a critical step towards addressing the climate challenges in Northwest Africa and fortifying the region's resilience in the face of climate change.

Keywords: Africa; Coastal wetlands; Climate change; Holocene; African Humid Period; Paleolimnology; Sedimentology.

56 INTRODUCTION

57 Climate change and its impacts on the environment and societies represent one of the most
58 significant challenges of this century. Africa is one of the most climate-vulnerable continents
59 due to the combined effect of its significant exposure to climate change and its low
60 socioeconomic adaptive capacity ¹. In the last decade, the northwest coast of Morocco has
61 been hit by severe winter storms and occasional cyclones, causing extensive damage to the
62 environment and society ².

63 Situated along Africa's northern tectonic plates, Morocco faces various meteorological and
64 seismic threats, including earthquakes ³, tsunamis ⁴, landslides ⁵, inundations ⁶, marine
65 storms ², and the impacts of rising sea levels due to global climate change ⁷. Marine winter
66 storms cause intense flooding, beach erosion, and severe damage to roads and tourist
67 facilities ². Morocco boasts a coastal zone that stretches for over 3,500 kilometers along the
68 Atlantic Ocean and the Mediterranean Sea, encompassing a maritime area of approximately
69 1.2 million square kilometers and a fishing potential estimated by the FAO (United Nations
70 Food and Agriculture Organization) at nearly 1.5 million tons, renewable every year ⁸. The
71 fishing sector in Morocco is the third most significant contributor to the national economy,
72 following only agriculture and tourism. The Atlantic coast of Morocco is under many human
73 pressures, including urban expansion, pollution, and excessive exploitation of coastal
74 resources ⁹. Furthermore, high-energy marine events, such as marine storms, are increasing
75 the stress in the region, leading to short-term inundation of coastal lowlands, posing a threat
76 to people's safety and infrastructure ¹⁰.

77 Therefore, a better understanding of climate change's impact, such as increased storminess,
78 on Moroccan coastal environments and population is needed. However, information on
79 climate change in Northwest Africa, and especially in the Atlantic Sahara, remains scarce,
80 especially from the point of view of long records covering important periods in the Earth's
81 climate history ¹¹.

82 While the Holocene is generally regarded as a period of relative climatic stability, the
83 transition from the mid to late Holocene was marked by significant environmental changes
84 ¹²⁻¹⁴. This shift in Africa represented the transition from the “African Humid Period” during
85 the early Holocene to a drier late Holocene phase ¹⁵. Influenced by enhanced summer
86 insolation over North Africa and the consequent latitudinal displacement and contraction of
87 the Intertropical Convergence Zone (ITCZ), the W Africa monsoonal system underwent a
88 shift in its northward extent ¹⁵⁻¹⁹. The West African monsoonal system was pivotal in
89 governing moisture transport to Northwestern Africa, triggering substantial alterations in the
90 hydrological cycle and vegetation cover ^{18,20}. Both models ^{21,22} and proxy-based
91 reconstructions ^{15,16,23} suggest that this shift led to an amplification of the monsoonal climate
92 system and its northward reach due to feedback mechanisms involving vegetation, soil ²⁴
93 and extended water bodies ²⁵.

94 However, several questions surrounding the aridification patterns in Northwest Africa during
95 the mid to late Holocene persist. These inquiries revolve around three key aspects: first, the
96 exact timing of this transition ^{15,16,26,27}; second, whether this shift towards arid conditions
97 was generally abrupt ^{18,21,28-30}, and finally, the extent of the monsoonal influence reaching
98 northward ^{28,31,32}. Clarifying these questions is vital for gaining a more comprehensive
99 understanding of the hydroclimatic dynamics during this significant period in the Holocene
100 and the environmental feedback.

101 North Africa is a pivotal region for examining the intricate connections between low-latitude
102 African monsoon systems and large-scale millennial climate change ³³. The
103 paleoenvironmental reconstruction of coastal deposits provides valuable insights into
104 climate change and sea level changes caused by global to regional-scale exogenic processes
105 ³⁴. The primary obstacle when it comes to researching Holocene paleoenvironments in arid
106 regions lies in the somewhat limited preservation potential of sediments ³⁵. This limitation
107 poses a significant challenge to creating a comprehensive climatic change record. For this

108 reason, rare records are found within the region ^{11,18,36,37} and even fewer are located by the
109 coast ^{38,39}, which underscore the importance of our specific record in the northwestern
110 Sahara region.

111 In this study, we employ a multiproxy approach to document the paleoenvironmental
112 transformations that have taken place in the Khnifiss Lagoon, located in southern Morocco,
113 over the past 3.5 thousand years Before Present (kyrs BP). By reconstructing the
114 paleoenvironment at this unique site, situated on the Saharan Atlantic coast, we aim to shed
115 light on the hydroclimatic dynamics during a pivotal climatic period: the transition from the
116 mid to late Holocene and the termination of the African Humid Period. Furthermore, the
117 strategic latitudinal position of the Khnifiss Lagoon allows us to assess the interplay of
118 Northern Hemisphere climate patterns and the low-latitude African monsoon system on the
119 hydro-climate of northwest Africa and their variability in the past. Herein, the
120 paleoenvironmental reconstruction of a coastal lagoon in NW Africa recorded the impact of
121 increased storminess over the region and a relative delay in the drying tendency after the
122 mid Holocene, revealing an apparent synchronization between those events and the
123 occurrence of cooling events in the North Atlantic. Given the lack of studies in this
124 important climatic region, we expect that our results will contribute to understanding
125 hydroclimate variability in the transition from mid- to late Holocene and improve climate
126 prediction models that could enhance sustainable development and climate change
127 adaptation.

128

129 **METHODS**

130

131 **The Khnifiss Lagoon**

132 Situated along the southern Atlantic coast of Morocco, the Khnifiss Lagoon (28°02'54" N,
133 12°13'66" W) stretches for 20 km in length, covering an expansive surface area of 65 km²
134 (Fig. 1a). The Khnifiss Lagoon, including its salt flats, is the second most important wetland
135 in Morocco and the only tidal lagoon in the desert zone, providing shelter for a highly
136 diverse fauna, including wintering birds ⁴⁰. Data from the Ramsar sheet indicate that
137 Khnifiss Park is home to several vulnerable or threatened species at the national or
138 international level.

139 This coastal lagoon presents a small and shallow basin and rare freshwater input originating
140 from the temporary river (*Oued*) Aouedri. The lagoon is connected to the Atlantic Ocean by
141 a perennial inlet known as *Foum Agoutir*, leaving the lagoon subject to tidal influence ⁴¹.

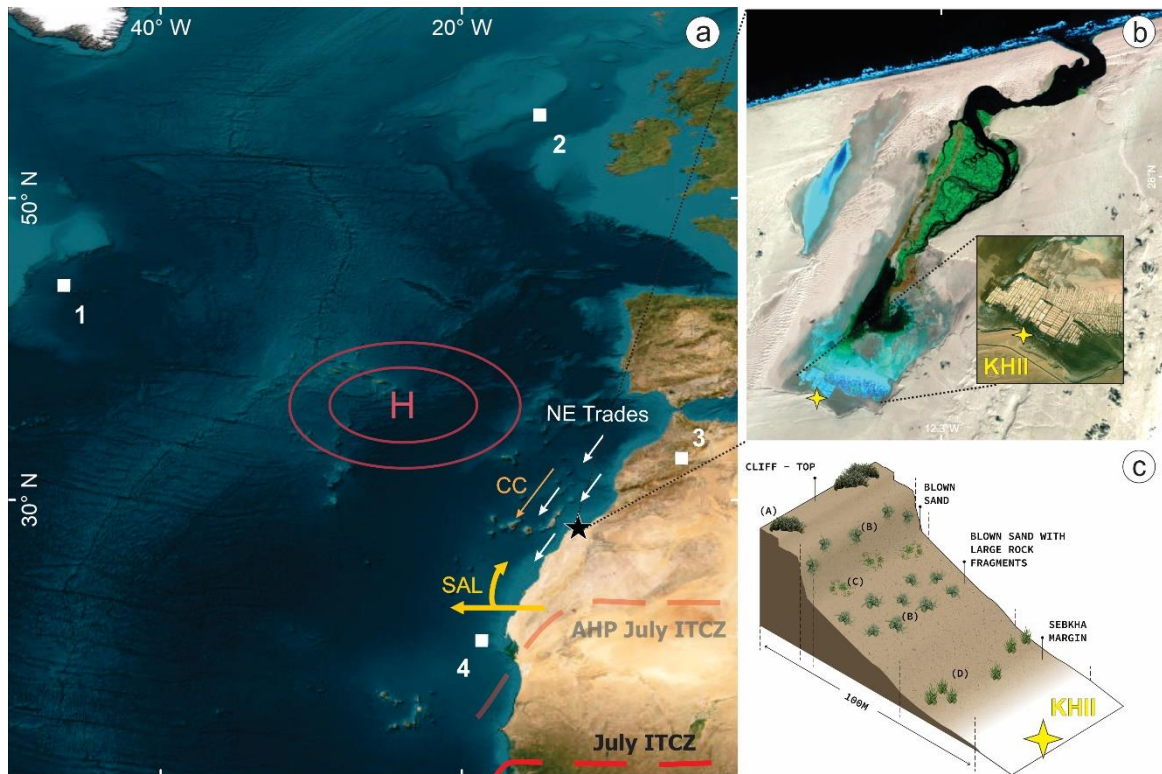
142 The lagoon features dendritic channels that fill progressively with the tides and narrow
143 upstream. The interconnected tidal channels are flanked by intertidal mudflats, a seagrass
144 bed (*Zoostera*), and an extensive tidal salt marsh, which only floods on the highest tides and
145 boasts a wide variety of vegetation. These salt marshes reveal a clear zoning pattern within
146 the tidal ecosystem, often attributed to the flora's resilience and adaptation to fluctuating
147 flood and salinity conditions.

148 The salt marsh extends upstream into the salt flat named *Sebkha Tazra*. However, due to its
149 distance from the inlet, most of *Sebkha Tazra* is unaffected by the tidal cycle and lacks
150 vegetation. During rare periods of rain or exceptionally high spring tides, *Sebkha Tazra* can
151 be briefly flooded ⁴². This extensive saltflat depression is enclosed by cliffs, and
152 groundwater lies close to its sandy floor. Due to this configuration, it is possible to observe a
153 thick salt crust formed after the evaporation of groundwater. In the northern and northeast
154 parts of *Sebkha Tazra*, we find transitional areas between salt marsh, desert reg, and salt flat,
155 where small communities of plants grow on small mounds of sand (Fig. 1c).

156 The Khnifiss Lagoon is under a hot desert climate (BWh), characteristic of dry, arid, low-
157 latitude deserts, according to the Köppen Climate Classification System. Previous works ⁴³⁻

158 ⁴⁵ describe southwestern Morocco under the influence of interannual to multidecadal
159 timescale climate changes and within the Saharan bioclimatic stage. Wind, humidity, and
160 precipitation in the region are associated with the North Atlantic Oscillation (NAO) phase
161 and the relative position of the Azores anticyclone, as it generates the trade winds that hit the
162 coast obliquely. The very same winds are associated with an important upwelling
163 phenomenon that occurs in the region of the Canary Current (CC), particularly near Cape
164 Ghir, as highlighted by previous research ⁴⁶ (Fig. 1a). A speleothem from southwestern
165 Morocco reveals a millennial long influence of both the NAO and the Atlantic Multidecadal
166 Oscillation (AMO) in the region ⁴⁴.

167 Previous research in the Khnifiss Lagoon suggests that, in the last century, the coast was
168 directly affected by NAO oscillations and sea level changes ⁴⁵. A combined approach with
169 remote sensing data and geochemical analysis reveals the sensitivity of the Khnifiss Lagoon
170 to large-scale climatic processes, such as NAO. During its positive phase, a strong east-to-
171 west wind leads to a widening of the inlet, which, in turn, affects the hydrodynamics and
172 biogeochemical cycles of the lagoon ⁴⁵. Previous studies indicate that the expansion of the
173 Khnifiss Lagoon and surrounding areas is governed by the inlet's dynamic, the sea level of
174 Morocco, and changes in the hydrological condition ^{45,47}. Therefore, our record has the
175 potential to improve further our knowledge of the climatic mechanisms and dynamics
176 influencing NW Africa environments during the last ~3.5 kyrs BP.



177 **Figure 1** – Geographical, climatic and ecological set of the Khnifiss Lagoon (black star). (a) Climatic
 178 mechanisms acting over south Morocco: CC (Canaries Current); SAL (Saharan Air Layer); latitudinal position
 179 of the Intertropical Convergence Zone (ITCZ) during winter in the present day (red dashed line) and in the
 180 African Humid Period (AHP; faded red dashed line); latitudinal position of the Azores High Pressure Zone (red
 181 H); (1) and (2) correspond to the marine cores presented by Bond et al.^{48,49} (MC52 + VM29191 and MC21 +
 182 GGC22), (3) Pollen reconstruction for the Atlas Mountain based on data from the sediment core at Lake
 183 Tigalmamine⁵⁰ (4) NW Africa Humidity Index marine sediment core GeoB7920²⁹. (b) The Khnifiss Lagoon
 184 remote sense image in the composition 543 where the vegetation (green), water (black) and salt flat (*sebkha*;
 185 blue) and the position of the KHII sediment core (yellow star) are highlighted. (c) vegetation distribution
 186 profile around the coring location.

187

188 Sediment core

189 To deepen our understanding of the region’s paleoclimatic dynamics and the changes in its
 190 paleoenvironment, we manually collected a sediment core from the innermost area of
 191 Sebkha Tazra in the Khnifiss Lagoon (KHII: 27°54 ‘55.1’ N, 12°22’04.4” W) (Fig. 1b).

192 Before opening, the sediment core was x-rayed using a Siemens 500 ma Polymat S Plus X-
 193 ray equipment operating at 85 kVp, 124 mA, 200 mAs. The gray scale of the image was
 194 generated using the software ImageJ. The sediment core was opened in half with a
 195 subsequent description of the most prominent visible features and the color following the
 196 Munsell chart. Subsequently, an X-ray fluorescence (XRF) analysis was performed using an

197 ARTAX Bruker AXS XRF spectrometer, operating at 25 kV and 500 mA, to obtain the
198 elementary mapping of the sample surface along the sediment core. The sediment core was
199 then sliced into 1-cm subsamples, and visible shells and other mineral specimens were
200 separated for further analysis.

201 The KHII sediment core was dated at the LMC14 Artemis Laboratory in Saclay, France,
202 according to the following methodology. Samples were treated in an excess of 0.5N
203 hydrochloric acid for several hours at 80°C to eliminate carbonates, then rinsed with
204 ultrapure water until neutral pH. Different quantities, depending on the % Total Organic
205 Carbon (TOC) of the samples, were taken to obtain, after combustion, a volume of CO₂
206 containing about 1 mg of carbon. The sample was burned in the presence of about 500 mg of
207 copper oxide and a silver wire for 5 hours at 835°C. The CO₂ was then reduced by hydrogen
208 in the presence of iron powder at 600°C. The mass of iron is equal to 3 times the mass of
209 carbon, with a minimum value of 1.5 mg and a maximum value of 4 mg. The carbon
210 deposited on the iron powder and the assembly was pressed into a support for measurement
211 by Accelerator Mass Spectrometry (AMS). The ¹⁴C activity of the sample was calculated by
212 comparing the sequentially measured intensities of the ¹⁴C, ¹³C, and ¹²C beams of each
213 sample with those of CO₂ standards prepared from the reference oxalic acid HOxII and
214 expressed in pMC (percent Modern Carbon) normalized to a deltaC13 of -25 per thousand.
215 Radiocarbon ages were calculated according to Mook and van der Plicht (1999) in
216 correcting the fractionation with the deltaC13 calculated from the ¹³C/¹²C ratio measured on
217 ARTEMIS. The deltaC13 used included fractionation during both sample preparation and
218 the SMA measurement. Measurement uncertainty accounted for both statistical error and
219 measurement variability for the sample and the subtracted blank.

220 To determine the origin of sedimentary organic matter, elemental and isotopic carbon
221 concentrations were analyzed in samples after acid attack (HCl 3%) to remove the carbonate
222 fraction. δ¹³C and organic carbon determination were performed in a FlashHT 2000

223 elemental analyzer coupled with a Delta V Advantage mass spectrometer from Thermo
224 Fisher Scientific with a precision of 0.05 per mil for $\delta^{13}\text{C}$ and 0.05% for organic carbon. The
225 $\delta^{13}\text{C}$ is expressed in per mil (‰) against the international standard VPDB (Vienna Pee Dee
226 Belemnite).

227 To determine the composition of three mineral specimens recovered from the sediment core,
228 finely crushed sub-samples were deposited on a flat silicon (Si) monocrystal support. X-ray
229 diffraction (XRD) patterns of the samples were recorded on a Panalytical X'Pert Powder
230 diffractometer equipped with a PIXcel detector (255 active channels) and Cu anticathode
231 operating at 40 kV and 40 mA. The diffractograms were measured in the 3° - 70° 2θ range
232 with a step size. Mineral identification was performed using Highscore 3.0 software and two
233 databases: ICSD (Inorganic Crystal Structure Database) and COD (Crystallography Open
234 Database).

235 Preserved specimens of mollusk shells, preferably whole, were separated for identification
236 during core subsampling. The samples were subjected to an ultrasonic bath for two rounds
237 of 1 minute using ultrapure water to remove the deposited material. Specimens were
238 identified by specialists at the Department of Zoology, Charles University (Czech Republic)
239 and at the Laboratory of Applied Geology and Geo-Environment, Ibn Zohr University
240 (Morocco), taking into account the species distribution at the Khnifiss Lagoon and later
241 photographed.

242 A principal component analysis (PCA) was performed using Statistica software by StatSoft
243 to support multi-proxy interpretation and discussion.

244

245

246

247 **RESULTS AND DISCUSSION**

248 **The Khnifiss Lagoon paleoenvironment in the last 3.5 kyr**

249 The 207 cm sediment core has shown clear zonation that reflects the paleoenvironmental
250 changes that occurred in the Khnifiss Lagoon (Fig. 2). To understand the timing of those
251 changes, we focused on the portion between 155 and 227 cm of depth and dated four key
252 positioned samples (160-161: 2769 ± 27 cal yrs BP, 185-186: 6587 ± 56 cal yrs BP, 202-203:
253 3442 ± 35 cal yrs BP and 218-219: 3428 ± 29 cal yrs BP). Dating of coastal lagoons inserted
254 in semi-/arid areas is challenging and outliers, as the one in sample 185-186, can be common
255 ^{10,52} mainly due to remobilization or periods of intense desiccation cycles. Although, we
256 acknowledge the limitations derived from the reduced number of ¹⁴C samples, we are
257 convinced that this chronology should not limit the analysis of the overall trend recorded
258 over the past ~3.5 kyrs and described as it follows.

259

260

261

262

263

264

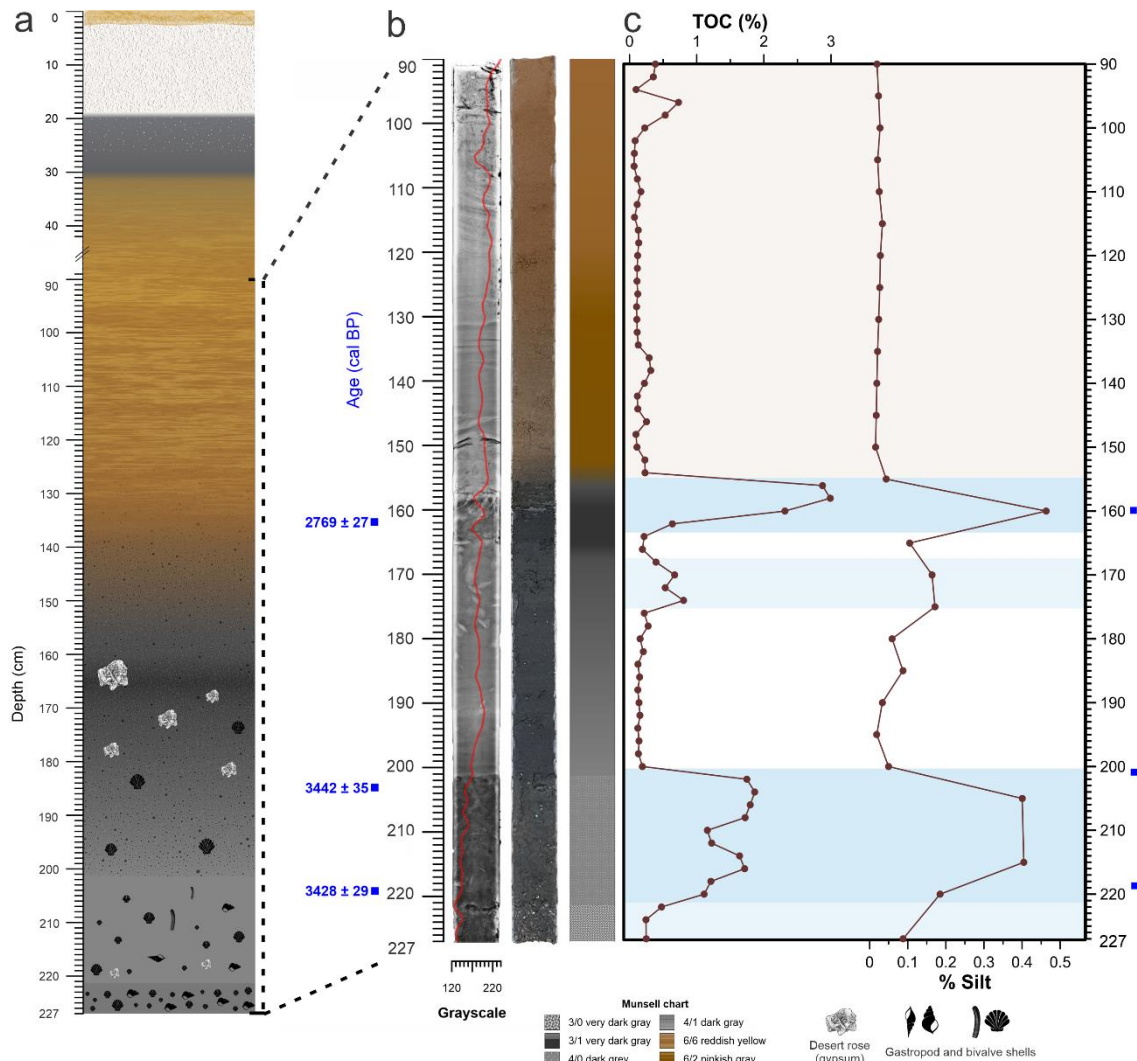
265

266

267

268

269



270 **Figure 2** – KHI sediment core profile (a), x-ray (b), photography, and (c) TOC and silt variation. Blue shading
 271 represents periods of higher humidity, while orange shading refers to dry periods.

272

273 The first phase, corresponding to the period before 3428 ± 29 cal yrs BP (221 – 227 cm),
 274 shows a continuous increase of COT ($\mu = 0.97\%$), C/N, and silt, followed by a decrease in
 275 salinity (Fig. 3), as indicated by the Sr/Ca ratio⁴⁵. In a previous study, the isotope and
 276 elemental signatures of vegetation within Khnifiss Park were reported (Nogueira et al.,
 277 2022). This information served as the basis for interpreting the C/N vs. $\delta^{13}\text{C}$, suggesting a
 278 combined contribution of submerged vegetation and phytoplankton. The abundant presence
 279 of mollusk shells (*Cerastoderma edule*, *Dosinea exoleta*, *Giberulla miliaria*,
 280 *Calliostomatidae*, and *Nasaridae*) suggests a perennial presence of water during this period.
 281 The mentioned species inhabit intertidal muddy sand flats and are also typically associated

282 with *Zoostera* grass beds. Granulometry during this period indicated a muddy sand substrate
283 characterized by poorly sorted grains that varied in the size of medium sand and very coarse
284 silt. The combined interpretation of the proxies points to an environment with a perennial
285 presence of water and a gradual development of pioneer marsh vegetation ⁴⁵. Therefore, a
286 progressive increase in water levels, the related drop in salinity, and the predominance of
287 marine dinoflagellate cysts may indicate a greater marine influence during this period.

288 The second phase, centered around 3435 ± 32 cal yrs BP (201 – 221 cm), shows an increase
289 in TOC ($\mu = 1.52\%$) content and a displacement towards higher C/N values. The C/N vs.
290 $\delta^{13}\text{C}$ diagram points to an increased contribution of eventually submerged salt marsh
291 vegetation. At the same time, the amount of titanium, here used as a proxy for silt/clay
292 minerals ⁵³, increases, reflecting changes in the soil possibly related to marsh development.
293 The large drop in salinity and the continuous presence of marine dinoflagellate cysts and
294 *Chenopodiaceae* pollen corroborate the interpretation of a well-developed salt marsh with
295 high marine influence, as also described for the lagoon Moulay-Boulsalham in north
296 Morocco ⁵⁴. Although less abundant, mollusks such as *Cerastoderma edule*, *Odostomia sp.*,
297 *Solen sp.*, *Turitella sp.*, Nassaridae, Mathildidae are still present and are known to typically
298 inhabit *Zostera* seagrass and intertidal zones, possibly indicating the low tide mark. In
299 general, during phase II there is an established salt marsh, with constant presence of water,
300 increased marine influence, and high sedimentation rate (20 cm deposited around 3435 ± 32
301 cal yrs BP).

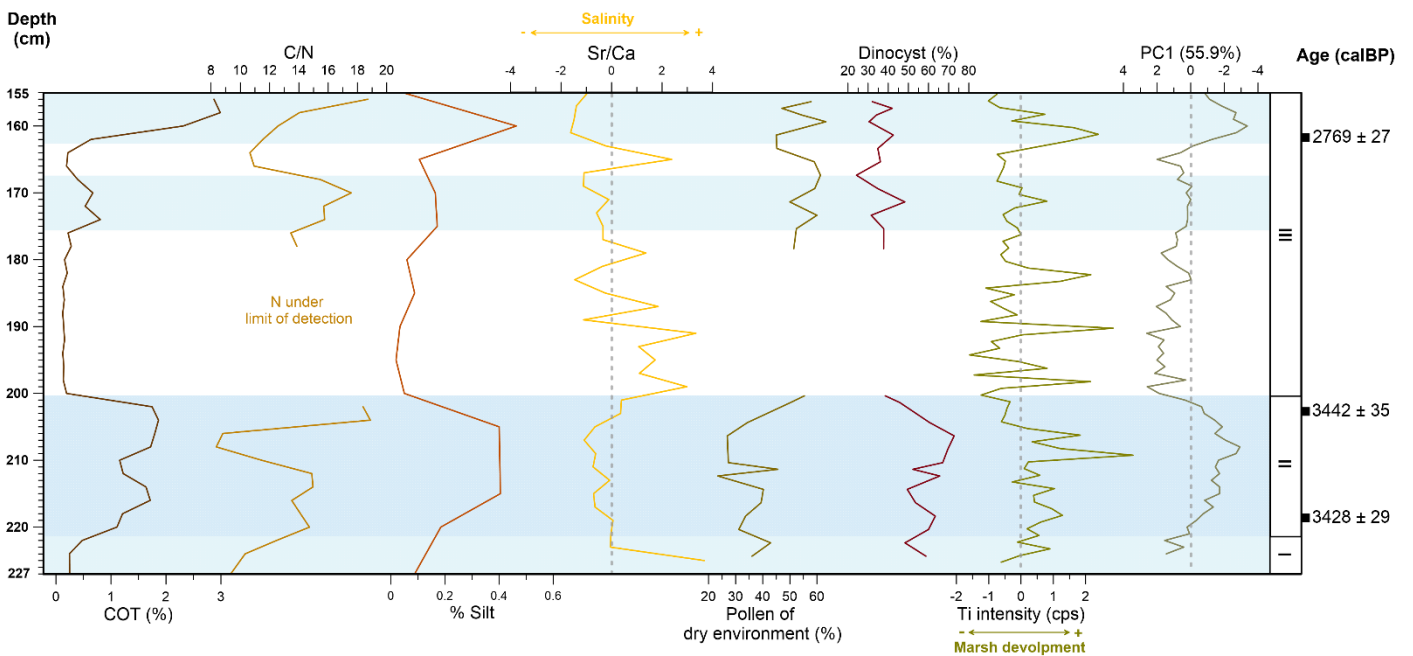
302 The third phase, which occurred between 3435 ± 32 cal yrs BP and $\sim 2769 \pm 27$ cal yrs BP
303 (155 – 201 cm), records a dramatic environmental change. At the beginning of this phase,
304 between 175 and 201 cm, a very low TOC ($\mu = 0.17\%$) is found, and nitrogen values are
305 lower than the detection limit. This could indicate a possible organic matter decomposition,
306 denitrification, and volatilization of nitrogen compounds as the lagoon, at this point, dries
307 out. Furthermore, no dinoflagellate cysts or pollens were found during this period. The grain

308 size analysis shows moderately well and moderately sorted fine and medium sand grains,
309 generally associated with a selective sedimentation agent, such as the wind. Indeed, the x-
310 ray image (Fig. 2b) reveals a lamination pattern of deposition during this phase. Aeolian-
311 deposited sand typically displays wind-ripple laminations characterized by planar-parallel
312 and undulatory layers and fine to medium grains⁵⁵. Thus, a predominant aeolian influence
313 was occurring at the distal point of the Khnifiss Lagoon during the beginning of the third
314 phase. The water would still arrive at this point, probably per percolation initially, and later,
315 towards the end of this phase, forming a shallow water column accompanied by a decrease
316 in salinity. Between 165 and 175 cm, it is possible to observe a significant number of
317 crystalline structures identified by DRX analysis as gypsum rosettes. The presence of these
318 minerals of evaporites is associated with rapid fluctuations of water in an arid environment
319 rich in CaSO₄, especially in shallow-water saline lakes and lagoons that go through repeated
320 cycles of dissection⁵⁶. During this phase, it is possible to observe two brief increases in
321 TOC: the first one centered around 173 cm and the second and highest one centered around
322 160 cm (i.e., around 2769 ±27 cal yrs BP) that are both accompanied by a drop in salinity.
323 These could indicate a brief return of marine influence, allowing a discreet salt marsh to
324 develop in the distal part of the lagoon. This interpretation is corroborated by the low
325 presence of dinocysts and the increased presence of pollens of dry environments. This phase
326 is abruptly interrupted in 2769 ± 27 cal yrs BP (30 – 155 cm) by dry conditions indicated by
327 a laminated reddish yellow (6/6) sand associated with aeolian transportation and deposition.
328 The well-sorted and rounded sand-grain population shows that the source of aeolian sand
329 may have become dominated by coastal dunes.

330 A thick layer of approximately 16 cm of salt covered by loose sand tops the laminated sand
331 (Figure 2a). The salt crust is then followed by a gray sticky silt layer (4/0 dark gray) of about
332 10 cm. This layer's average organic carbon content is 0.51%, except for the most recent
333 layer, which presents 2.17%. The presence of crust and grey silt is due to variations in

334 groundwater level, which is linked to variations in local rainfall, sea level, and hydrological
 335 changes ⁵⁷.

336 In summary, in contrast to the established *Sebkha* seen today, a developed salt marsh was
 337 present $\sim 3435 \pm 32$ cal yrs BP and $\sim 2769 \pm 27$ cal yrs BP, indicating an advance in the
 338 marine influence even in the most continental portions of the lagoon. The current arid
 339 condition, therefore, was only completely established after 2769 ± 27 cal yrs BP. These
 340 significant shifts in environmental parameters highlight the dynamic nature of the region's
 341 ecosystem during these particular timeframes.



342 **Figure 3** – KHII's main proxies' profile and phases.

343

344 **Holocene Climate Variability and Coastal Responses in Northwest Africa**

345 In the present days, during the boreal winter season, the characteristics of storms, including
 346 their location, intensity, and frequency in the North Atlantic, are predominantly influenced
 347 by the dynamics of the jet stream and the atmospheric pressure systems within the region.

348 This relationship is elucidated by the NAO index, with anomalies correlated to fluctuations
 349 in solar activity, notably in ultraviolet radiation ⁵⁸. In the positive phase of the NAO,

350 intensified westerly winds push the storm track northward, directing it towards northern
351 Europe. Consequently, this region witnesses warmer and wetter conditions, while northern
352 Africa and southern Europe face drier-than-normal weather. Conversely, during the negative
353 phase, the storm tracks shift southward, resulting in increased precipitation in the western
354 Mediterranean and northern Africa and causing northern Europe to experience colder and
355 drier conditions than usual ⁵⁹⁻⁶¹.

356 Throughout the Holocene, both models and paleoclimate reconstructions have indicated that
357 orbital changes led to a progressively steeper temperature gradient and an overall northward
358 shift in the storm track towards the present days ⁶⁰⁻⁶⁴. In the late Holocene, the northern
359 hemisphere witnessed recurring cooling events, as documented by Bond et al. ⁶⁵. These
360 events, potentially linked to reduced solar irradiance, may have given rise to a scenario
361 reminiscent of a negative phase of the NAO. This climatic pattern, a consequence of the
362 interplay of atmosphere-ocean dynamics, resulted in increased precipitation and storm
363 activity across southern Europe and North Africa ⁶⁶. Data from a marine core retrieved off
364 the coast of western Africa (at 20° N) indicates that the Holocene climatic cycles closely
365 paralleled synchronous changes in Sea Surface Temperature (SST), emphasizing a strong in-
366 phase relationship between high- and low-latitude climates ¹⁵.

367 Our sediment core has documented two periods of salt marsh expansion in the most inland
368 portions of the Khnifiss Lagoon in 3.5 kyrs BP (event 1 = E1) and 2.7 kyrs BP (event 2 =
369 E2). Coastal wetlands in arid regions can respond to changes in the i) relative sea level; ii)
370 fluvial apport variation; iii) precipitation amount; iii) wind structure linked to the tidal inlet
371 dynamics; and iv) extreme events such as tsunamis and storms ^{45,67-70}. At the ebb-dominated
372 Khnifiss Lagoon, previous studies indicated that when storm surges are directed to the
373 continent, increased wave energy causes an enhanced hydraulic slope in the flooding tide
374 within the inlet channel, leading to a net landward movement of sediment and water. This
375 process culminates in the upbuilding of the flood tidal delta – with the deposition of higher

376 grain size – and in the washover of smaller grain size sediments on the salt marsh, allowing
377 its development and expansion ^{45,47,69,71}. A comprehensive analysis, incorporating both
378 remote sensing data and geochemical assessments, has provided a detailed account of the
379 dynamics within the Khnifiss Lagoon over the past century. This investigation has suggested
380 varying degrees of sensitivity to climatic events depending on the proximity to the lagoon's
381 inlet. Notably, the more inland regions of the lagoon appear to be impacted solely by
382 significant climatic events ⁴⁵.

383 To comprehend the dynamics behind progradation events E1 and E2, we conducted a
384 Principal Components Analysis (PCA) using data on TOC content, Sr/Ca ratio, silt content,
385 and Ti from KHII. Notably, the first principal component accounted for a significant 56% of
386 the explained variance, as shown in Figure 5a, and revealed a distinct pattern characterized
387 by alternating phases of decrease and increase, which decreases were linked to salt marsh
388 accretion. These data are in agreement with different paleoenvironmental studies carried out
389 on the Moroccan Atlantic coast (Fig. 5b) that show high-energy-deposited-sediments
390 occurring at the same time as E1 and E2, suggesting a regional forcing causing these marine
391 transgressions. These on-shore deposits were reported in the form of fine sediments layers at
392 the estuaries of Tahaddart (35.5° N) ^{10,72} and Loukkos (35.15° N) ⁴ and at the Moulay-
393 Bousalham (34°N) and Oualidia (32°N) lagoons ^{38,39,54}, and marine gastropods shells
394 deposited at Moulay Douraine (31° N) ⁷³. Biogeographic evidence from the NW African
395 coast (28 – 19° N) suggests a transgression event taking place around 3.5 kyrs BP ⁷⁴, also
396 recorded by wetlands on the Atlantic coast of Spain in addition to another one around 2.8
397 kyrs BP ⁷⁵⁻⁷⁷. Changes in Holocene vegetation in France and southwest Spain indicate a
398 humid period between 3.4 and 2.8 kyrs BP, with two arid phases (4.3 – 3.4 kyrs BP and 2.8 –
399 1.7 kyrs BP) flanking it ⁷⁸ (Jalut et al. 2000). Along the Portuguese coast, a humid period
400 occurred around 3 kyrs BP, interrupting the drier conditions that preceded and followed it ⁷⁹.
401 Flood frequency records from northeastern Morocco also point to increased precipitation

402 between 3.2 and 2.7 kyrs BP ⁸⁰. In the western Mediterranean, increased precipitation
403 recorded around 3.3 and 2.7 kyrs BP ⁶⁶ coincided with low NAO stages ⁸¹. Both simulations
404 ²⁵ and paleo records ^{18,28,29,32,52,82–84} indicate humid conditions in the northern Africa around
405 3 kyrs. On a millennial timescale, coastal areas' sediments can become more or less likely to
406 record overwash deposition according to variations of relative sea level, inlet(s) position and
407 size, and sediment supply changes ^{10,85,86}. This can lead to variations in the record of events'
408 frequency and intensity in the sediments, resulting in potential delays or omissions when
409 comparing these events across different environments. Nevertheless, the sediment records
410 along the Morocco, Iberian Peninsula, and the Mediterranean point to high-energy events
411 and humid conditions around 3.5 kyrs and 2.8 kyrs BP, impacting as south as 27° N. For the
412 Khnifiss Lagoon, the E2 relative lower sedimentation, when compared to E1, and the
413 abundance of gypsum rosettes during this period are climatically influenced and are a
414 consequence of the rising aridity trend observed in Morocco ⁸⁷ (Fig. 5c) and NW Africa in
415 general ²⁹ (Fig. 5d) that may have limited the saltmarsh accretion. Peak synchronism among
416 the Khnifiss Lagoon and other proxy records, as evident in Figure 5, indicates an influence
417 of storm surges that probably caused the inlet opening and widening and water to arrive
418 even in the most distant parts of the lagoon. In combination with a more humid climate, the
419 salt marsh thrived in this portion of the lagoon during these events; however, once drier
420 conditions settled in, the marsh gave way to a salt flat, present until these days.

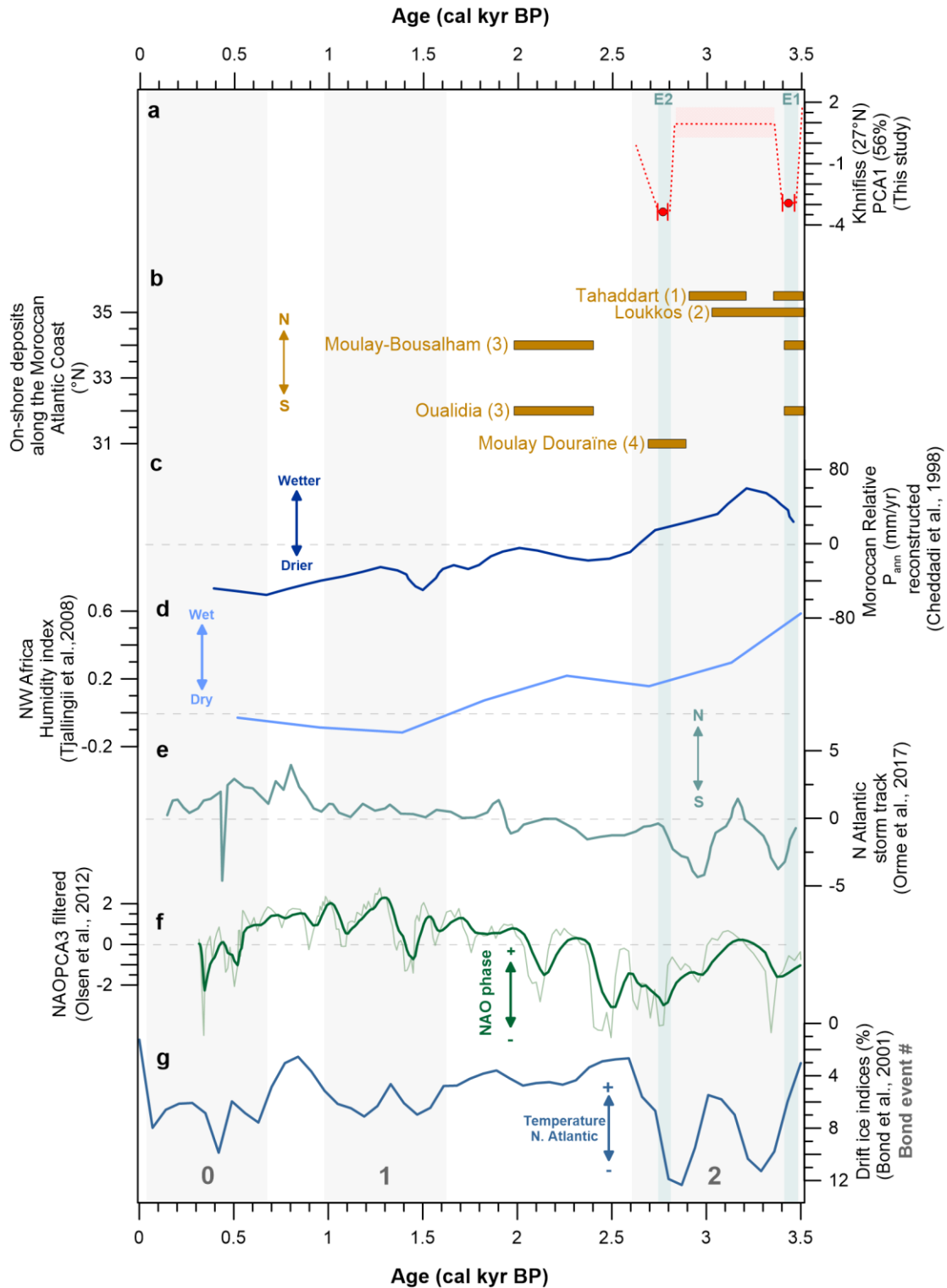
421 Currently, the climate in our study region is dominated by the baroclinic variation over the
422 North Atlantic ⁸⁸, and therefore, we hypothesize that our record can be compared to proxies
423 from higher latitudes in the northern hemisphere. Between 3.5 kyrs BP and 2.6 kyrs BP,
424 proxy records point to low temperatures in the Northern Hemisphere, as suggested by the
425 stacked record of Ice-Rafted Debris (IRD) reconstructed in the North Atlantic (Bond #2)¹⁴.
426 During the late Holocene, the cooling observed in the North Atlantic region may be
427 attributed to atmospheric-ocean dynamics, including changes in the strength of sub-tropical

428 gyres, as previously explained. This cooling increased precipitation over Northwestern
429 Africa and the Mediterranean, causing a southward shift in the storm tracks. These changes
430 are reflected in the North Atlantic storm index (Fig. 5e; ⁶⁴). This climatic scenario is
431 comparable with the present NAO negative phase ⁸⁹ and is evident in the reconstructed
432 Holocene NAO index⁸¹ (Fig. 5f) and pointed out previously⁸². When reviewing paleoclimate
433 records from diverse global regions, researchers have pinpointed up to six noteworthy
434 periods of rapid climate change (RCC) within the Holocene. A distinct cooling trend in polar
435 regions marked these RCC events. Among these, one particularly significant RCC event
436 unfolded between 3.5 and 2.5 kyrs BP ^{12,14} that may have been linked with the negative
437 NAO-like scenarios that impacted northwest Africa.

438 The termination of the African Humid Period (AHP) has been the subject of debate within
439 the scientific community, with most studies convergent on an overall abrupt climatic change
440 occurring at ~5.5 kyrs BP ^{15,18,90,91}. However, few other studies favor a more gradual
441 transition ^{21,28,29}. The Khnifiss Lagoon, located at 27°N, currently has a climate dominated
442 by the North Atlantic climate system ⁸⁸. However, during the Holocene, this latitude
443 represented the boundary between a dominance by this system at north and a monsoonal
444 climate system dominance at south ¹⁸. In the transition from mid- to late Holocene, this
445 region was under the influence of the northernmost expansion of the West African Summer
446 Monsoon (WASM) ^{11,28,31,32,36,83}. Therefore, the Khnifiss Lagoon's core, with its sensitivity
447 to the interplay of these two climatic systems, supports the idea of a gradual climate
448 transition in Northwest Africa's coastal regions and records humid conditions until ca 2.7
449 kyrs BP. This observation agrees with other studies that suggest that a humid period can be
450 clearly recognized from about 5 kyrs BP to 3 kyrs BP in North Africa ⁹² and until 2 kyrs BP
451 in south Morocco ⁹³. Hence, we claim that the proposed prolongation of wetter conditions in
452 the Atlantic Sahara was a consequence of the combination of i) RCC events characterized by
453 polar cooling that may have caused an NAO-like scenario that triggered the southward

454 migration and weakening of the Azores High and storminess over north Africa and ii) a
455 northward expansion of the West African Summer Monsoon (WASM). These conditions
456 sustain the concept of a possible teleconnection between hydrological conditions over
457 Northwest Africa and the North Atlantic climatic variability. On a smaller scale, our work, in
458 conjunction with Nogueira et al. ⁴⁵, highlights the resilience of coastal wetlands to climate
459 fluctuations. It underscores the significant influence of humidity conditions, particularly in
460 arid regions, on salt marsh accretion and inland expansion.

461 Anticipated global warming may reduce the temperature gradient in mid- to high latitudes,
462 causing winter storm tracks to shift southward and increasing the frequency of storms along
463 Morocco's Atlantic coast ⁶⁴. Enhancing our knowledge of the environmental feedback to
464 these changes is crucial in minimizing uncertainties associated with such shifts, which is
465 essential for effective climate adaptation strategies.



466 **Figure 4** – (a) Khnifiss first principal component (PCA1, 56%) compared to (b) other on-shore deposits along
 467 the Moroccan Atlantic coast at: (1) Tahaddart estuary¹⁰, (2) Loukkos estuary⁴, (3) Moulay-Bousalham and
 468 Oualidia coastal lagoons³⁹ and (4) Moulouya Douraine⁹⁴; (c) Moroccan relative precipitation reconstruction
 469 based on pollen records⁵⁰; (d) NW Africa Humidity index²⁹; (e) North Atlantic storm track reconstruction⁶⁴;
 470 (f) North Atlantic Oscillation (NAO) reconstruction⁸¹ and (g) North Atlantic drift ice indices⁴⁸. Vertical gray
 471 bars and numbers represent the different Bond events while green vertical bars mark the timing of high energy
 472 events (Event 1: E1, Event 2: E2) recorded at the Khnifiss Lagoon.

473

474

475 CONCLUSION

476 The challenges posed by climate change in Morocco and Northwest Africa are significant
477 and multifaceted. The region grapples with environmental and societal threats like storms,
478 earthquakes, and rising sea levels, all exacerbated by urbanization and resource exploitation.

479 The research conducted in the Khnifiss Lagoon serves as a valuable window into the
480 transition from the mid to late Holocene, shedding light on the intricate relationship between
481 climate patterns in the North Atlantic and the climate in NW Africa.

482 The paleoenvironmental reconstruction in the Khnifiss Lagoon has revealed a
483 synchronization between increased storminess and delayed aridification in NW Africa and
484 cooling events in the North Atlantic during the mid- to late Holocene transition. As
485 previously suggested by other researchers, a negative NAO-like scenario could be
486 responsible for such circumstances in south Morocco. At the same time, these conditions
487 must have delayed the aridification trend in the north Saharan coastal environments, which
488 only started after about 2.7 kyrs BP. This suggests that the African Humid Period
489 termination, usually regarded as ca 5.5 kyrs BP, must have happened at different times
490 across North Africa due to environmental specificities. More research on the exact time and
491 nature of these changes, extending the knowledge further back in the past with high
492 resolution archives is needed to understand the extension of the impacts and the climatic
493 feedback between NW Africa and conditions in the North Atlantic.

494 The emphasis on understanding the dynamic interplay between climate fluctuations and
495 coastal environments highlights the resilience and adaptability of these regions. With the
496 specter of global warming on the horizon, research focusing on predicting possible changes
497 in storm patterns along Morocco's Atlantic coast is necessary. These findings can potentially
498 enhance climate prediction models, offering opportunities to better prepare for and adapt to
499 the evolving climate patterns in the region. Overall, the knowledge gained from these studies

500 represents a critical step towards addressing the climate challenges in Northwest Africa and
501 fortifying the region's resilience in the face of climate change.

502

503 REFERENCES

- 504 1. Niang, I. *et al.* Africa. in *Climate Change 2014: Impacts, Adaptation and Vulnerability - Contributions*
505 *of the Working Group II to the Fifth Assessment Report of the Intergovernmental Panel on Climate*
506 *Change*. 1199–1265 (Cambridge University Press, 2014).
- 507 2. Mhammdi, N. *et al.* Marine storms along the Moroccan Atlantic coast: An underrated natural hazard?
508 *J. African Earth Sci.* **163**, 103730 (2020).
- 509 3. Cherkaoui, T. & El Hassani, A. Seismicity and Seismic Hazard in Morocco 1901-2010. *Bull. l'Institut*
510 *Sci.* **34**, 45–55 (2012).
- 511 4. Mhammdi, N. *et al.* Sedimentary evidence of palaeo-tsunami deposits along the Loukkos estuary
512 (Moroccan Atlantic Coast). *Journal Tsunami Soc. Int.* **34**, 83–100 (2015).
- 513 5. Harmouzi, H. *et al.* Landslide susceptibility mapping of the Mediterranean coastal zone of Morocco
514 between Oued Laou and El Jebha using artificial neural networks (ANN). *Arab. J. Geosci.* **12**, 696
515 (2019).
- 516 6. *Wadi Flash Floods*. (Springer Singapore, 2022). doi:10.1007/978-981-16-2904-4.
- 517 7. Satta, A., Snoussi, M., Puddu, M., Flayou, L. & Hout, R. An index-based method to assess risks of
518 climate-related hazards in coastal zones: The case of Tetouan. *Estuar. Coast. Shelf Sci.* **175**, 93–105
519 (2016).
- 520 8. Royaume du Maroc. *Portrait de secteur de pêche maritime au Maroc*. (2015).
- 521 9. Snoussi, M., Khouakhi, A. & Niang-diop, I. Geomorphology Impacts of sea-level rise on the Moroccan
522 coastal zone : Quantifying coastal erosion and flooding in the Tangier Bay. **107**, 32–40 (2009).
- 523 10. Khalfaoui, O., Dezileau, L., Degeai, J. P. & Snoussi, M. A late Holocene record of marine high-energy
524 events along the Atlantic coast of Morocco: new evidences from the Tahaddart estuary.
525 *Geoenvironmental Disasters* **7**, (2020).

- 526 11. Ait Brahim, Y., Bouchaou, L. & Wanaim, A. Speleothem-based paleoclimate research in South
527 Morocco: Interest and perspectives. *Front. Sci. Eng.* **11**, 9–16 (2021).
- 528 12. Mayewski, P. a. *et al.* Holocene climate variability. *Quat. Res.* **62**, 243–255 (2004).
- 529 13. Haug, G. H. Southward Migration of the Intertropical Convergence Zone Through the Holocene.
530 *Science (80-.)*. **293**, 1304–1308 (2001).
- 531 14. Bond, G. *et al.* Persistent solar influence on north atlantic climate during the Holocene. *Science (80-.)*.
532 **294**, 2130–2136 (2001).
- 533 15. deMenocal, P. *et al.* Abrupt onset and termination of the African Humid Period: *Quat. Sci. Rev.* **19**,
534 347–361 (2000).
- 535 16. Claussen, M., Kubatzki, C., Brovkin, V. & Ganopolski, A. Simulation of an abrupt change in Saharan
536 vegetation in the mid-Holocene. *Geophys. Res. Lett.* **26**, 2037–2040 (1999).
- 537 17. Haug, G. H., Hughen, K. A., Sigman, D. M., Peterson, L. C. & Röhl, U. Southward migration of the
538 intertropical convergence zone through the holocene. *Science (80-.)*. **293**, 1304–1308 (2001).
- 539 18. Kuhlmann, H., Meggers, H., Freudenthal, T. & Wefer, G. The transition of the monsoonal and the N
540 Atlantic climate system off NW Africa during the Holocene. *Geophys. Res. Lett.* **31**, 1–4 (2004).
- 541 19. McGee, D., Donohoe, A., Marshall, J. & Ferreira, D. Changes in ITCZ location and cross-equatorial
542 heat transport at the Last Glacial Maximum, Heinrich Stadial 1, and the mid-Holocene. *Earth Planet.*
543 *Sci. Lett.* **390**, 69–79 (2014).
- 544 20. Kuhlmann, H., Freudenthal, T., Helmke, P. & Meggers, H. Reconstruction of paleoceanography off
545 NW Africa during the last 40,000 years: Influence of local and regional factors on sediment
546 accumulation. *Mar. Geol.* **207**, 209–224 (2004).
- 547 21. Tierney, J. E., Pausata, F. S. R. & DeMenocal, P. B. Rainfall regimes of the Green Sahara. *Sci. Adv.* **3**,
548 (2017).
- 549 22. Jolly, D., Harrison, S. P., Damnati, B. & Bonnefille, R. Simulated climate and biomes of Africa during
550 the late Quaternary: Comparison with pollen and lake status data. *Quat. Sci. Rev.* **17**, 629–657 (1998).
- 551 23. Shanahan, T. M. *et al.* Atlantic forcing of persistent drought in West Africa. *Science (80-.)*. **324**, 377–
552 380 (2009).

- 553 24. Claussen, M., Dallmeyer, A. & Bader, J. *Theory and Modeling of the African Humid Period and the*
554 *Green Sahara*. vol. 1 (Oxford University Press, 2017).
- 555 25. Specht, N. F., Claussen, M. & Kleinen, T. Simulated range of mid-Holocene precipitation changes
556 from extended lakes and wetlands over North Africa. *Clim. Past* **18**, 1035–1046 (2022).
- 557 26. Kröpelin, S. *et al.* Climate-Driven Ecosystem Succession in the Sahara: The Past 6000 Years. *Science*
558 *(80-.)*. **320**, 765–768 (2008).
- 559 27. Blois, C., Forman, S. L. & Wright, D. K. Water level history for Lake Turkana, Kenya in the past
560 15,000 years and a variable transition from the African Humid Period to Holocene aridity. *Glob. Planet.*
561 *Change* **132**, 64–76 (2015).
- 562 28. Höpker, S. N. *et al.* Pronounced Northwest African Monsoon Discharge During the Mid- to Late
563 Holocene. *Front. Earth Sci.* **7**, 1–17 (2019).
- 564 29. Tjallingii, R. *et al.* Coherent high- and low-latitude control of the northwest African hydrological
565 balance. *Nat. Geosci.* **1**, 670–675 (2008).
- 566 30. Armitage, S. J., Bristow, C. S. & Drake, N. A. West African monsoon dynamics inferred from abrupt
567 fluctuations of Lake Mega-Chad. *Proc. Natl. Acad. Sci.* **112**, 8543–8548 (2015).
- 568 31. Faure, H. Changements climatiques au sud des régions méditerranéennes: le Sahara et le Sahel au
569 Quaternaire. in *Quaternary climate in Western Mediterranean* (ed. Lopez-Vera, F.) 533–534
570 (Universidad Autónoma, 1986).
- 571 32. Wengler, L. & Vernet, J. L. Vegetation, sedimentary deposits and climates during the Late Pleistocene
572 and Holocene in eastern Morocco. *Palaeogeogr. Palaeoclimatol. Palaeoecol.* **94**, 141–167 (1992).
- 573 33. Weldeab, S., Lea, D. W., Schneider, R. R. & Andersen, N. 155,000 Years of West African Monsoon
574 and Ocean Thermal Evolution. *Science (80-.)*. **316**, 1303–1307 (2007).
- 575 34. Ghandour, I. M. *et al.* Mid-Late Holocene Paleoenvironmental and Sea Level Reconstruction on the Al
576 Lith Red Sea Coast, Saudi Arabia. *Front. Mar. Sci.* **8**, 1–20 (2021).
- 577 35. Ritchie, J. C., Eyles, C. H. & Haynes, C. V. Sediment and pollen evidence for an early to mid-
578 Holocene humid period in the eastern Sahara. *Nature* **314**, 352–355 (1985).
- 579 36. Sha, L., Brahim, Y. A., Wassenburg, J. A., Yin, J. & Peros, M. How Far North Did the African
580 Monsoon Fringe Expand During the African Humid Period? Insights From Southwest Moroccan

- 581 Speleothems Geophysical Research Letters. 93–102 (2019) doi:10.1029/2019GL084879.
- 582 37. Baqloul, A. *et al.* Climate and land-use effects on hydrological and vegetation signals during the last
583 three millennia: Evidence from sedimentary leaf waxes in southwestern Morocco. *Holocene* **31**, 699–
584 708 (2021).
- 585 38. Raynal, J. & Ballouche, A. Nouvelles données sur la formation des systèmes lagunaires atlantiques
586 marocains pendant le cycle mellahien. (1985) doi:10.13140/RG.2.1.2517.3928.
- 587 39. Ballouche, A. & Carruesco, C. Evolution holocène d'un écosystème lagunaire : la lagune de Oualidia
588 (Maroc atlantique). *Rev. géologie Dyn. géographie Phys.* **27**, 113–118 (1986).
- 589 40. Beaubrun, P.-C., Thevenot, M. & Schouten, J. R. Wintering and summering water bird populations in
590 the Khnifiss Lagoon. in *The Khnifiss lagoon and its surrounding environment (Province of L'ayoune,*
591 *Morocco)* (eds. Dakki, M. & Ligny, W. de) 125–140 (Trav. Inst. Sci., 1988).
- 592 41. Dakki, M. & Ligny, W. de. *The Khnifiss lagoon and its surrounding environment (Province of*
593 *L'ayoune, Morocco)*. *Trav. Inst. Sci.* (1988).
- 594 42. Dakki, M. & Parker, D. M. The Khnifiss Lagoon and adjacent desert area: geographical description
595 and recent coastline changes. in *The Khnifiss lagoon and its surrounding environment (Province of*
596 *L'ayoune, Morocco)* (eds. Dakki, M. & Ligny, W. de) 2–6 (1988).
- 597 43. Idrissi, J. L. *et al.* Organisation et fonctionnement d'un écosystème côtier du Maroc : la lagune de
598 Khnifiss. *Rev. des Sci. l'eau* **17**, 447–462 (2004).
- 599 44. Ait Brahim, Y. *et al.* Speleothem records decadal to multidecadal hydroclimate variations in
600 southwestern Morocco during the last millennium. *Earth Planet. Sci. Lett.* **476**, 1–10 (2017).
- 601 45. Nogueira, J. *et al.* Coastal wetland responses to a century of climate change in northern Sahara,
602 Morocco. *Limnol. Oceanogr.* **67**, 285–299 (2022).
- 603 46. McGregor, H. V, Dima, M., Fischer, H. W. & Mulitza, S. Rapid 20th-Century Increase in Coastal
604 Upwelling off Northwest Africa. *Science (80-.)*. **315**, 637–639 (2007).
- 605 47. Agbani, M. A. El, Fekhaoui, M., Bayed, A. & Schouten, J. R. The Khnifiss Lagoon and adjacent
606 waters: hydrology and hydrodynamics. in *The Khnifiss Lagoon and its surrounding environment*
607 *(Province of La'youne, Morocco)* (eds. Dakki, M. & Ligny, W. de) 17–26 (Trav. Inst. Sci., 1988).
- 608 48. Bond, G. *et al.* Persistent Solar Influence on North Atlantic Climate During the Holocene. *Science (80-*

- 609 .). **294**, 2130–2136 (2001).
- 610 49. Bond, G. *et al.* A pervasive millennial-scale cycle in North Atlantic Holocene and glacial climates.
611 *Science* (80-.). **278**, 1257–1266 (1997).
- 612 50. Cheddadi, R., Lamb, H. F., Guiot, J. & Van Der Kaars, S. Holocene climatic change in Morocco: A
613 quantitative reconstruction from pollen data. *Clim. Dyn.* **14**, 883–890 (1998).
- 614 51. Mook, W. G. & van der Plicht, J. Reporting 14 C Activities and Concentrations. *Radiocarbon* **41**, 227–
615 239 (1999).
- 616 52. Ndiaye, A. *et al.* Reconstruction of the holocene climate and environmental changes of Niayes peat
617 bog in northern coast of Senegal (NW Africa) based on stable isotopes and charcoals analysis. *Quat.*
618 *Sci. Rev.* **289**, 107609 (2022).
- 619 53. PannoZZo, N., Smedley, R. K., Plater, A. J., Carnacina, I. & Leonardi, N. Novel luminescence
620 diagnosis of storm deposition across intertidal environments. *Sci. Total Environ.* **867**, 161461 (2023).
- 621 54. Ballouche, A., Lefevre, D., Carruesco, C., Raynal, J. P. & Texier, J. P. Holocene environments of
622 coastal and continental Morocco. *Quat. Clim. West. Mediterr.* 517–531 (1986)
623 doi:10.13140/2.1.1724.7529.
- 624 55. Winsemann, J., Hartmann, T., Lang, J., Fälber, R. & Lauer, T. Depositional architecture and
625 aggradation rates of sand-rich, supercritical alluvial fans: Control by autogenic processes or high-
626 frequency climatic oscillations? *Sediment. Geol.* **440**, (2022).
- 627 56. Torfstein, A., Gavrieli, I., Katz, A., Kolodny, Y. & Stein, M. Gypsum as a monitor of the paleo-
628 limnological-hydrological conditions in Lake Lisan and the Dead Sea. *Geochim. Cosmochim. Acta* **72**,
629 2491–2509 (2008).
- 630 57. Parker, D., Bell, R. & Pye, S. Soils of the coastal platform between Khnifiss Lagoon and Tarfaya. in
631 *The Khnifiss Lagoon and its surrounding environment (Province of La'youne, Morocco)* (eds.
632 Mohamed Dakki & Ligny, W. De) 172 (Trav. Inst. Sci., 1988).
- 633 58. Martin-Puertas, C. *et al.* Regional atmospheric circulation shifts induced by a grand solar minimum.
634 *Nat. Geosci.* **5**, 397–401 (2012).
- 635 59. Hurrell, J. W. Decadal Trends in the North Atlantic Oscillation: Regional Temperatures and
636 Precipitation. *Science* (80-.). **269**, 676–679 (1995).

- 637 60. Orme, L. C. *et al.* Aeolian sediment reconstructions from the Scottish Outer Hebrides: Late Holocene
638 storminess and the role of the North Atlantic Oscillation. *Quat. Sci. Rev.* **132**, 15–25 (2016).
- 639 61. Goslin, J. *et al.* Holocene centennial to millennial shifts in North-Atlantic storminess and ocean
640 dynamics. *Sci. Rep.* **8**, 1–12 (2018).
- 641 62. Brayshaw, D. J., Hoskins, B. & Black, E. Some physical drivers of changes in the winter storm tracks
642 over the North Atlantic and Mediterranean during the Holocene. *Philos. Trans. R. Soc. A Math. Phys.*
643 *Eng. Sci.* **368**, 5185–5223 (2010).
- 644 63. Bakke, J., Lie, Ø., Dahl, S. O., Nesje, A. & Bjune, A. E. Strength and spatial patterns of the Holocene
645 wintertime westerlies in the NE Atlantic region. *Glob. Planet. Change* **60**, 28–41 (2008).
- 646 64. Orme, L. C. *et al.* Past changes in the North Atlantic storm track driven by insolation and sea-ice
647 forcing. *Geology* **45**, 335–338 (2017).
- 648 65. Bond, G. *et al.* A Pervasive Millennial-Scale Cycle in North Atlantic Holocene and Glacial Climates.
649 *Science (80-.)*. **278**, 1257–1266 (1997).
- 650 66. Zielhofer, C. *et al.* Western Mediterranean hydro-climatic consequences of Holocene ice-rafted debris
651 (Bond) events. *Clim. Past* **15**, 463–475 (2019).
- 652 67. Deaton, C. D., Hein, C. J. & Kirwan, M. L. Barrier island migration dominates ecogeomorphic
653 feedbacks and drives salt marsh loss along the Virginia Atlantic Coast, USA. *Geology* (2017)
654 doi:10.1130/G38459.1.
- 655 68. Schuerch, M. *et al.* Future response of global coastal wetlands to sea-level rise. *Nature* (2018)
656 doi:10.1038/s41586-018-0476-5.
- 657 69. Roman, C. T., Peck, J. A., Allen, J. R., King, J. W. & Appleby, P. G. Accretion of a New England
658 (U.S.A.) salt marsh in response to inlet migration, storms, and sea-level rise. *Estuar. Coast. Shelf Sci.*
659 (1997) doi:10.1006/ecss.1997.0236.
- 660 70. Więski, K., Guo, H., Craft, C. B. & Pennings, S. C. Ecosystem Functions of Tidal Fresh, Brackish, and
661 Salt Marshes on the Georgia Coast. *Estuaries and Coasts* **33**, 161–169 (2010).
- 662 71. FitzGerald, D. M. Shoreline Erosional-Depositional Processes Associated with Tidal Inlets. *Hydrodyn.*
663 *Sediment Dyn. Tidal Inlets* **29**, 186–225 (1988).
- 664 72. Khalfaoui, O. *et al.* Paleoenvironmental evolution and evidence of marine submersion events from

- 665 mid-to late Holocene in northwestern Morocco: The case of the Tahaddart lower estuary. *Cont. Shelf*
666 *Res.* **256**, 104958 (2023).
- 667 73. Weisrock, A. L. E. Late-middle pleistocene, late pleistocene and holocene palaeo-sea-level records at
668 agadir and the atlantic atlas coastal reach,morocco: An updated overview. *Quaternaire* **23**, 211–225
669 (2012).
- 670 74. Petit-Maire, N. Holocene biogeographical variation along the northwestern African coast (28 - 19 N).
671 in *Sahara and the surrounding areas* (eds. Sarnthein, M., Seibold, E. & Rognon, P.) 365–377
672 (Balkema, 1980).
- 673 75. Zazo, C. *et al.* The coastal archives of the last 15ka in the Atlantic–Mediterranean Spanish linkage
674 area: Sea level and climate changes. *Quat. Int.* **181**, 72–87 (2008).
- 675 76. Lario, J. *et al.* Holocene palaeotsunami catalogue of SW Iberia. *Quat. Int.* **242**, 196–200 (2011).
- 676 77. Ruiz, F. *et al.* Geomorphology Sedimentological and geomorphological imprints of Holocene tsunamis
677 in southwestern Spain : An approach to establish the recurrence period. *Geomorphology* **203**, 97–104
678 (2013).
- 679 78. Jalut, G., Esteban Amat, A., Bonnet, L., Gauquelin, T. & Fontugne, M. Holocene climatic changes in
680 the Western Mediterranean, from south-east France to south-east Spain. *Palaeogeogr. Palaeoclimatol.*
681 *Palaeoecol.* **160**, 255–290 (2000).
- 682 79. Santos, L., Sánchez-Goñi, M. F., Freitas, M. C. & Andrade, C. Climatic and environmental changes in
683 the Santo André coastal area (SW Portugal) during the last 15,000 years. in *Quaternary climatic*
684 *changes and environmental crises in the Mediterranean Region* 175–179 (2003).
- 685 80. Zielhofer, C., Bussmann, J., Ibouhouten, H. & Fenech, K. Flood frequencies reveal Holocene rapid
686 climate changes (Lower Moulouya River, northeastern Morocco). *J. Quat. Sci.* **25**, 700–714 (2010).
- 687 81. Olsen, J., Anderson, N. J. & Knudsen, M. F. Variability of the North Atlantic Oscillation over the past
688 5,200 years. *Nat. Geosci.* **5**, 808–812 (2012).
- 689 82. Holz, C., Stuut, J. B. W., Henrich, R. & Meggers, H. Variability in terrigenous sedimentation processes
690 off northwest Africa and its relation to climate changes: Inferences from grain-size distributions of a
691 Holocene marine sediment record. *Sediment. Geol.* **202**, 499–508 (2007).
- 692 83. Kim, J. H. *et al.* Impacts of the North Atlantic gyre circulation on Holocene climate off northwest

- 693 Africa. *Geology* **35**, 387–390 (2007).
- 694 84. Bouimetarhan, I. *et al.* Palynological evidence for climatic and oceanic variability off NW Africa
695 during the late Holocene. *Quat. Res.* **72**, 188–197 (2009).
- 696 85. Woodruff, J. D., Irish, J. L. & Camargo, S. J. Coastal flooding by tropical cyclones and sea-level rise.
697 *Nature* **504**, 44–52 (2013).
- 698 86. Dezileau, L. *et al.* Intense storm activity during the Little Ice Age on the French Mediterranean coast.
699 *Palaeogeogr. Palaeoclimatol. Palaeoecol.* **299**, 289–297 (2011).
- 700 87. Cheddadi, R., Lamb, H. F., Guiot, J. & Van Der Kaars, S. Holocene climatic change in Morocco: A
701 quantitative reconstruction from pollen data. *Clim. Dyn.* **14**, 883–890 (1998).
- 702 88. Knippertz, P., Christoph, M. & Speth, P. Long-term precipitation variability in Morocco and the link to
703 the large-scale circulation in recent and future climates. *Meteorol. Atmos. Phys.* **83**, 67–88 (2003).
- 704 89. Jalali, B., Sicre, M.-A., Azuara, J., Pellichero, V. & Combourieu-Nebout, N. Influence of the North
705 Atlantic subpolar gyre circulation on the 4.2 ka BP event. *Clim. Past* **15**, 701–711 (2019).
- 706 90. McGee, D., deMenocal, P. B., Winckler, G., Stuut, J. B. W. & Bradtmiller, L. I. The magnitude, timing
707 and abruptness of changes in North African dust deposition over the last 20,000 yr. *Earth Planet. Sci.*
708 *Lett.* **371–372**, 163–176 (2013).
- 709 91. Collins, J. A. *et al.* Rapid termination of the African Humid Period triggered by northern high-latitude
710 cooling. *Nat. Commun.* **8**, 1372 (2017).
- 711 92. Roberts, N. *The Holocene: an environmental history.* (John Wiley & Sons, 2014).
- 712 93. Weisrock, A. *Geomorphologie et Paléoenvironnements de l'Atlas atlantique, Maroc.* (Notes et Memoires
713 du Service Geologique du Maroc, 1993).
- 714 94. Weisrock, A. *Geomorphologie et paléoenvironnements de l'Atlas atlantique, Maroc.* (Universite Paris I
715 Pantheon-Sorbonne, 1980).
- 716
- 717